Lithographic Processing of Polymers Using Plasma-Generated Electron Beams

LUMIN LI, JAYARAM KRISHNASWAMY, ZENGQI YU, SENIOR MEMBER, IEEE, GEORGE J. COLLINS, FELLOW, IEEE, HIROYUKI HIRAOKA, AND MARY ANN CAOLO

Abstract—**Pattern definition in polymer films is achieved using electron beams generated in soft vacuum (0.05–0.50 torr) glow discharges either on a continuous or pulsed (20–100 ns) basis. With the continuous-mode electron beam, 7-μm transmission mask features are replicated in both polymethyl methacrylate (PMMA) and polyimide resists. Using a pulsed electron-beam submicron (~ 0.5 μm) features are transferred from an electron-transmitting stencil mask into the PMMA. The soft-vacuum pulsed electron beam is also eminently suited for polymer stabilization. Pulsed electron-beam hardening of 0.05–3.5-μm-thick AZ-type and MacDermid resist patterns is also demonstrated with hardened resist patterns stable to temperatures between 200° and 350°C. The demonstrated replication and pattern stabilization technique may be applicable in microelectronics packaging lithography where the resist thickness is substantial, linewidths are 1–10 μm, and registration requirements are less stringent.**

I. INTRODUCTION

SERIAL, DIRECT-WRITE electron-beam lithography is unsurpassed for achieving submicron feature sizes. However, the high cost and low wafer throughput of serial direct-write equipment are also restrictive disadvantages [1]. Previously developed parallel-write lithographic approaches [2] have problems with either the transmission mask or the wide-area electron source.

In electron-beam lithography, usually after electron exposure of the pattern, a subsequent wet or dry development process is used to delineate the relief image features in the polymer film. The simplest dry development scheme is self-development; i.e., spontaneous relief pattern replication upon exposure. For electron-induced self-development to occur, resist formulations with both higher electron-beam sensitivity and electron-induced volatization properties are required. One serious limitation to the use of high sensitivity resists in conventional electron-beam lithography is the evolution of polymeric vapors that degrade the performance of thermonic electron emitters (that use hot filaments in high vacuum). Bowden and Thompson [3] showed spontaneous relief formation on exposure to electron beams from fractured chains of poly(olefin-sulfones); molecular "unzipping" mechanisms were shown in polypthaldehydes by Ito and Wilson [4]. In some cases, post-exposure thermal assistance was needed, as shown by Hiraoka [5] and Yamada *et al.* [6]. Alternative approaches to self-development are the plasma dry development of previously exposed regions [7]–[9] and direct laser ablation [10].

Besides pattern delineation and possibly self-development, electron-beam processing has other applications to the lithographic process. There is a need to maintain both vertical etch profiles and critical dimensions [11] during subsequent high-temperature processes such as reactive ion etching, ion implantation, lift-off processes, and metal deposition. These issues are especially critical for images made in positive resist that exhibit more outgassing, reticulation, edge-rounding, and reflow during subsequent high-temperature process steps. Polymer stabilization can be achieved by electron-beam cross-linking as shown in this paper.

Both wet chemical [12] as well as other methods [13]–[22] of resist hardening have been proposed and demonstrated. UV hardening [13], [17], [18] of both photoresists and electron-beam resists is increasingly used [21]. Hiraoka and Pacansky [13] have used UV photons to thermophysically harden AZ-type photoresists. Orvek and Dennis [18] have shown the possibility of cross-linking films of the Shipley S1400-31 resist up to 1.5 μm in thickness using simultaneous UV radiation and heat energy. But UV photohardening is not suitable for hardening thicker layers because of high optical extinction in the UV for most organic groups ($\alpha = 0.5\text{–}1.0 \times 10^4$ L/mol cm), where 95% of the UV energy is absorbed within 300 nm of the surface of most resists [23] and nonuniform exposure versus depth occurs for thick resists. Poor electrical-to-photon conversion efficiency ($\sim 10^{-3}$), the limited operating lifetime (~ 1000 h) of ultraviolet lamps, and the requirement to filter out the IR component from the lamp spectrum further adds to the cost and complexity of this method.

Plasmas using various gas ambients have also been used to harden resist layers. In PRIST (Plasma Resist Image Stabilization Technique) [14], [20], the chemistry of the resist is modified by the bombardment of the resist surface using reactive and charged species produced in a fluoro-

Manuscript received April 3, 1989; revised November 4, 1989. This work was supported by the National Science Foundation (Quantum Electronics Waves and Beams) under Contract No. ECS-8815051, the Colorado Advanced Technology Institute, the Hewlett Packard Corporation, the Applied Electron Corporation, the IBM Corporation, and by M/S Buckbee-Mears of St. Paul, MN.

L. Li, Z. Yu, and G. J. Collins are with the Department of Electrical Engineering, Colorado State University, Fort Collins, CO 80523.

J. Krishnaswamy is with the Department of Material Science and Engineering, North Carolina State University, Raleigh, NC 27607.

H. Hiraoka is with IBM Almaden Research Center, San Jose, CA 98120.

M. A. Caolo is with the Hewlett Packard Corporation, Fort Collins, CO 80525.

IEEE Log Number 9034469.

carbon plasma. The strong reticulation (wrinkling) following the PRIST process indicates that the plasma primarily modifies only a very thin superficial layer because of low electron and ion energies in the plasma. Their penetration depth can at best equal those of the deep UV process. Plasma-assisted resist hardening prior to ion implantation has been reported by Johnson *et al.* [21] and Moran and Taylor [22] in O_2 and N_2 plasmas, respectively. Ion-beam hardening [15] is also depth-limited, even at 100-kV ion energy, due to the shallow penetration depth into polymer films. Furthermore, the use of ions may lead to the introduction of undesired contaminants into the underlying substrate.

High-energy electron-beam hardening systems, because of the deeper penetrating power and broader straggle of energetic electrons, allows for more uniform exposure versus depth. For example, 25-keV electrons penetrate a polymer resist with a density of 1.2 g/cm^3 to a depth of ~ 11 μm [25]. Despite the fundamental advantages of greater penetration depth and straggle, several practical disadvantages have restricted the use of previously reported electron-beam hardening systems. During resists hardening over a wide area, the production of volatile vapors reduces the thermonic emission efficiency and decreases the cathode life.

Herein, a photoresist patterning and associated polymer-hardening process using an electron beam produced in a glow discharge plasma [19], [24] is described.[1,2] The soft-vacuum processes described herein depart sharply from conventional techniques [1]–[3] in the following ways:

1) The large electron flux available from soft-vacuum electron guns allows for the self-development of a variety of polymers. Self-development in soft vacuum greatly reduces cathode contamination problems, since the cold cathodes used for electron production are highly tolerant, not only to process produced vapors but also to produce the background gas, including reactive gases.

2) For a stencil-mask-based lithographic system, soft-vacuum exposure has two important advantages: First, mask cooling is increased because of natural convective cooling. Secondly, mask charging is negligible because of the charge neutralization by background plasma ions.

3) The process takes place in dynamic soft vacuum where large pumping speeds are available for removing gases created by large-area electron exposure. The high pumping speeds in soft vacuum, which can greatly exceed product production rates, favor rapid removal of polymer products from the reactor which otherwise would contaminate the cathode.

The apparatus and processes are best suited for packaging lithography which uses thick (>5 μm) resist layers and where registration requirements are relaxed so that transmission mask alignment is not critical. Using a cold cathode to emit electrons allows for exposure over large areas with greatly reduced contamination concerns, relaxed vacuum requirements due to operation in soft vacuum, and a simple, reliable, and versatile apparatus.

[1]An electron beam curing/stabilization system is commercially available from Electron Vision Corporation, San Diego, CA.

[2]U.S. Patent applications for apparatus and process are pending.

II. Plasma-Generated Electron-Beam Source

A. Electron-Beam Source Apparatus and Operation

During discharge the electrons leave the cathode sheath region with nearly the entire cathode voltage. For the high E/P plasma conditions (E = electric field, and P = pressure) that are characteristic of the soft-vacuum electron-beam generation sheath (140 kV/cm-torr), Dreicer's condition [26] for highly directional electrons is satisfied and beam electrons are produced. The capability of electron-beam generation in soft vacuum is due to a combination of: (a) Cold cathode electron emission and sheath acceleration to form a directional beam, and (b) the large mean free path of beam electrons between gas collisions (15 mm) [27] compared to the small mask-substrate spacing ($=25$ μm). As they traverse the chamber volume they can undergo collisions with gas species that degrade their energy spectrum toward lower energies. However, the energy transfer in each of these collisions is small (tens of electronvolts) and the beam electrons remain very energetic and directional. The energy spectrum of the transmitted soft-vacuum electron beam, which impinges on the polymer surface, depends on the total gas pressure, the gas species, the composition of the cathode, the applied voltage, and the location from the cathode surface at which the energy spectrum is measured [28].

Fig. 1 illustrates the experimental apparatus of the continuous soft-vacuum electron-beam processing system, including the electron gun, vacuum chamber and proximity mask-alignment technique employed for polymer patterning. The electron-beam propagates from the cathode and past the ring anode to impinge onto the polymer film. To improve uniformity of the beam intensity anode, aperturing is used to allow only the central 2-cm diam portion of the electron beam launched from the 3.8-cm diam cathode to impinge on the substrate. Beam uniformity issues are further discussed in Section II-B.

A schematic diagram of the pulsed electron-beam apparatus is shown in Fig. 2. The pulsed electron beam emerges from the cathode with a diameter of 3.5 cm, is transmitted through the gas and impinges on the polymer film on the substrate. High peak electron-beam current density (>1 A/cm^2) is achieved from the cathode surface, as previously reported by Ranea-Sandoval [29], O'Brien [30], and Isaacs *et al.* [31]. The discharge chamber is evacuated to a pressure of less than 1 mtorr and then backfilled with either helium or filtered dry air to 50 mtorr. A 25-kV negative pulse is applied to the cathode to initiate the discharge. When using an energy storage capacitor of 7.5nF charged to 25 kV, a volumetric discharge which lasts for about 100 ns is produced. The temporal characteristics of these pulses have been measured. Fig. 3(a) shows a typical pulsed discharge current waveform measured with a Tektronix 7104 scope on a 1-MΩ

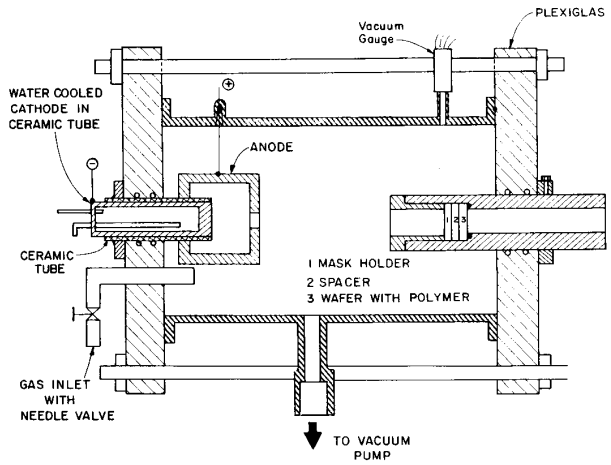

Fig. 1. Exposure and self-development system for polymer films, including the dc soft-vacuum electron-beam source, vacuum chamber, and the proximity mask to the wafer alignment apparatus.

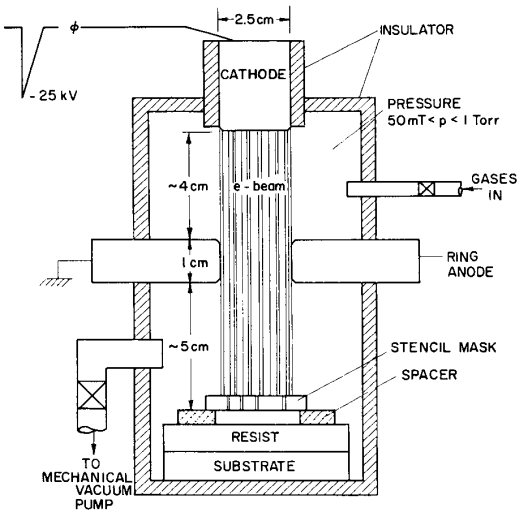

Fig. 2. Pulsed soft-vacuum electron-beam proximity exposure apparatus, including the cold cathode, ring anode, stencil mask/spacer, and substrate.

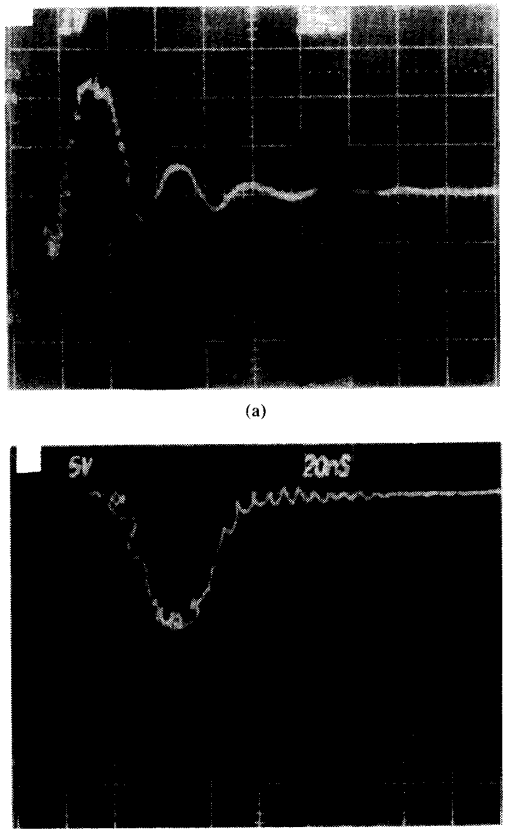

(a)

(b)

Fig. 3. (a) Soft-vacuum electron-beam discharge current wave form. (b) Discharge voltage measured between the ground terminal and cold cathode.

input terminal using a short rise-time current transformer. The first peak rises to ~3.75 kA in about 20 ns. Fig. 3(b) shows the voltage measured between the cathode and ground terminal using a voltage divider for fast-rising voltages. For a charging voltage of 25 kV the discharge peak is approximately 22 kV. The current and voltage signals are noisy due to the unshielded measuring environment.

B. Spatial Profiles of Electron Beams

Three-dimensional spatial profiles of plasma-created electron beams were measured under both cw and pulsed conditions using a movable Faraday probe with a small opening. An apertured graphite cover placed in front of the Faraday cup detector sets the spatial resolution during beam profiling to ± 0.2 mm. Electrons and ions from the beam-created plasma diffuse and impinge on the beam detector to cause undesired errors in the measured electron-beam current. To reduce these errors, the narrow sampling hole of the detector shield must be used to filter out most ions and electrons from the plasma and obtain adequate spatial resolution. To further reduce undesired background plasma currents, the detector shield is grounded, while the detector is placed at a retarding potential of -1.5 V to reject those plasma electrons of kinetic energy less than ~1.5 eV impinging the beam detector. The electron-beam profile measurements were done in soft-vacuum conditions and at distances from the cathode similar to those used during polymer processing. The intensity profile of the cw electron beam versus position across the beam for three different interelectrode distances (2.6, 5.1, and 7.6 cm) are shown in Fig. 4 at an air pressure of 100 mtorr and a gun voltage of 3 kV. A sharp beam-intensity peak appeared in the center of the beam profile for the anode located at 2.6 cm from the cathode, while it flattened out as the anode was moved away from the cathode due to gas scattering.

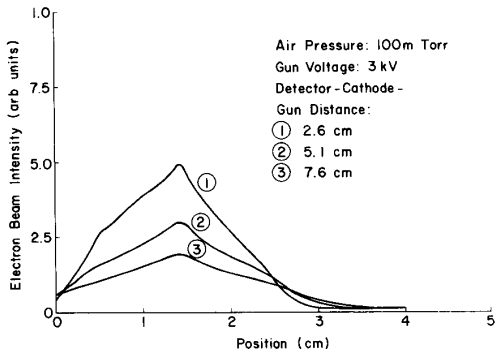

Fig. 4. Intensity profile of the dc electron beam at cathode–anode distances of 2.6, 5.1, and 7.6 cm.

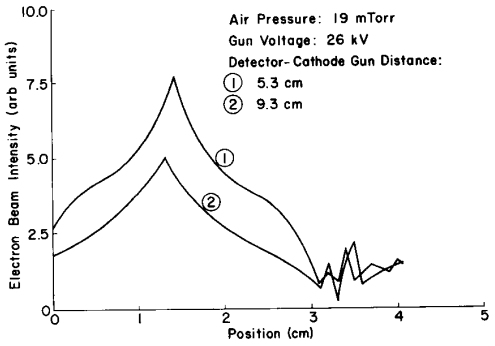

Fig. 5. Pulsed electron-beam intensity profiles at 5.3- and 9.3-cm cathode to detector spacings.

Pulsed electron-beam intensity profiles versus position across the beam for a variety of beam propagation distances were also measured. Fig. 5 shows beam intensity profiles recorded at various distances from the cold cathode. A sharp central peak in the intensity profile occurs and flattens only slightly with increasing distance from the cathode, as shown in Fig. 5. (The observed structure at greater than 3 cm is caused by an undesired edge discharge.)

In all exposure studies given below, the anode–cathode spacing never exceeded 8 cm. Moreover, resist patterning and hardening properties were measured over only a 2-mm diam sampling area to remove ambiguities due to the nonuniform beam profile. The intensity profiles shown in Figs. 4 and 5 are clearly very nonuniform. In the present study, the resist was exposed to a 2-mm-diam hole in which the electron intensity is approximately uniform over the small area. For further large-area application, the intensity uniformity can be dramatically improved by proper cathode design. This cathode tailoring goes beyond the intent of this paper. However, to illustrate the capability of beam profile control we show that the intensity profile from an optimized line-source electron beam is used in an electron beam recrystalization process, as shown in Fig. 6. The beam intensity uniformity of several percent intensity uniformity over 10-cm lengths is possible. The constant operating conditions used in this study are a total $He–O_2$ pressure of 500 mtorr and a 5% partial oxygen concentration. The optimization of operating conditions can be performed for the large-area cold cathodes used in the present study.

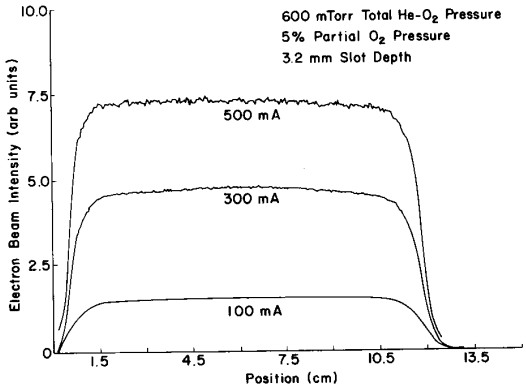

Fig. 6. Line-source electron-beam intensity profile versus the length along the cathode.

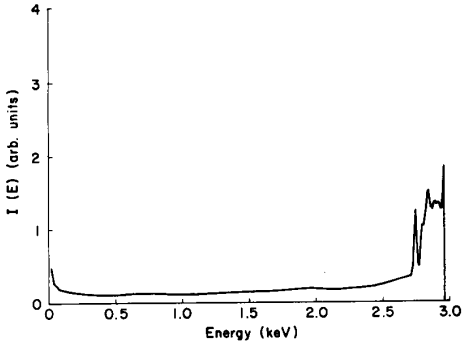

Fig. 7. Transmitted soft-vacuum electron-beam energy distribution.

C. Electron-Beam Energy Distribution

The transmitted electron-beam energy spectrum $I(E)$ impinging on the polymer was measured using a Faraday cup detector with the retarding potential technique [32]. Fig. 7 shows a typical $I(E)$ spectrum measure at a location which was 3 cm from a cold cathode electron gun for a cathode voltage of 2.96 kV in helium at 0.6 torr. The Faraday cup sampling chamber is differentially pumped by a turbomolecular pump to achieve a pressure in the detector below 10^{-5} torr. The Faraday detector is biased with a negative potential to filter-out electrons whose energy is less than the applied bias. The transmitted electron-beam energy distibution $I(E)$ can then be obtained by digitally differentiating the measured Faraday cup detector current with respect to the retarding potential. The resulting energy distribution curve can be divided into three regions: A low energy region ($E < 30$ eV), a minimally populated mid-energy band ($30 < E < 2700$ eV), and a high energy ($E = 2.7 \sim 3$ KeV) region which contains the electron beam. Electrons in the beam have a

maximum energy near eV_{max}, where V_{max} is the voltage applied to the cold cathode electron gun. Detailed Faraday cup experiments [33] have demonstrated that the density of high-energy beam electrons decreases with the total operating pressure, partial O_2 concentration, and the detector-to-cathode gun distance. The changes in the beam energy spectrum as it propagates through the gas is caused by the collisions between beam electrons and the gas medium. In a pure O_2 ambient, the high-energy beam electron component is dramatically reduced when compared to the operation in helium. This is also the case in rare gases other than in helium and at pressures above 20 torr.

A numerical simulation model to calculate the electron energy distribution of transmitted beam electrons created by the glow discharge electron gun both inside the cathode sheath and in the field free region [28] has been reported previously, with good agreement between experiment and simulation under cw conditions. The space-dependent Boltzmann equation has been numerically solved in this modeling, while the electron–electron and electron–atom collisions are included. Electrons gain their energy from the accelerating field at the cathode fall and redistribute their energy through collisions. The $I(E)$ changes versus the distance from the cathode, calculated by this model for the discharge conditions used for the present processing, are shown in Fig. 8 for operating in 100-mtorr helium and at a gun voltage of 4 kV. The simulation shows that the low-energy electrons are scattered out of the beam before their arrival at the transmission mask. In fact, the low-energy electron component, even at the sheath edge, is small compared to the high-energy beam component. Both experimental results and simulations indicate that the polymer exposure/self-development process, as well as the polymer hardening studies, are driven primarily by the high-energy component of the electron energy distribution.

D. Pulsed Electron Beam Dose Measurement on Polymers

The dose per pulse delivered to the polymer by the pulsed beam was measured using a calibrated radiochromic material [34] and consists of an organic dye in a nylon matrix. Using the calibrated film density at 510 nm (for the particular film used), the electron dose can be calculated. A piece of radiochromic film was exposed to 27.5-kV electron beams in 40 mtorr of dry air at a film-to-cathode separation of 8 cm. The radiochromic film used is 51-μm-thick, while the range of 27.5-kV electrons in nylon is 13.1 μm. The 51-μm-thick film saturates at a change in film density ΔD (measured at 510 nm) of 1.0, which sets the saturation value per micrometer of nylon at 0.0196 $\Delta D/\mu$m. For a film exposed by a single pulse of 27.5-keV electrons, the measured value of ΔD is 0.20. However, because the electrons are stopped in 13.1 μm, the $\Delta D/\mu$m is 0.0152, which is below the saturation level of the film. For two pulses, the value of ΔD is 0.32 and the value of $\Delta D/\mu$m is 0.024, which is above saturation. The mean density of two single-pulse exposures was measured to be 0.20. This corresponds to a measured dose of 2×10^6 rd by referring to a well-established calibration curve [34]. The current density of 27.5-keV electrons required to produce this dose was calculated to be 10.9 A/cm^2, corresponding to an incident charge dose of 1.09 μC/cm^2. A critical assumption in the above calculation is that the energy of electrons is solely 27.5 keV.

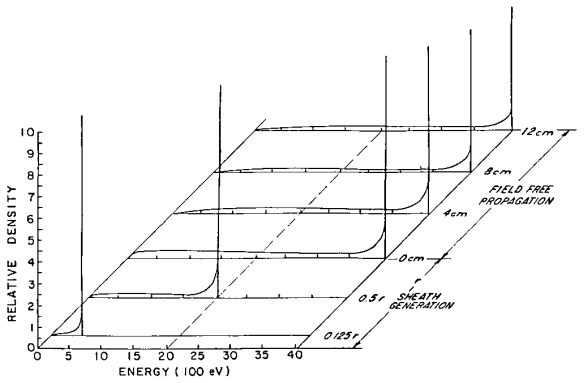

Fig. 8. Calculated electron energy spectrum of a glow discharge electron beam. Experimental conditions are 100-mtorr helium and 4-keV gun voltage.

III. Experimental Results

A. Resist Patterning by Continuous Electron-Beam Exposure

Typical continuous electron-beam operating conditions for the lithographic experiments performed in the apparatus of Fig. 1 are listed in Table I.

The polymer films used in our experiments were deposited by the spin-coating of polymer solutions on silicon substrates, followed by baking. When exposed to the electron beam, polymers, such as PMMA, Krylon, and polyamic acid, are etched away. The etching characteristics were investigated as a function of the discharge current and process gas. The removal rate of polymer is linear with the discharge current in the experimental regime [9]. A higher polymer removal rate is achieved in helium as compared to that found in nitrogen or argon at the same discharge current. This is attributed to both the greater beam transmission and the higher electron energy obtained in helium [33]. Hence, with all other conditions being the same, a larger electron dose reaches the polymer in a helium ambient. Although fewer high-energy beam electrons are present in pure O_2 than in pure helium for the same discharge current, the polymer removal rates in O_2 and air are higher than those in helium, argon, and nitrogen. This is attributed to the fact that oxygen plays an important chemical role in polymer removal. A residual gas analyzer (RGA) was used to measure the effect of the flow rate of oxygen on PMMA etching in a pure O_2 ambient. At high O_2 flow rates (140 sccm) the peak O_2 content is unchanged during the exposure, while at lower flow rates (4 sccm) the observed O_2 intensity shows a transient decrease about 1 min after the start of the ex-

TABLE I
EXPERIMENTAL CONDITIONS FOR ESTABLISHING CW ELECTRON BEAM

Gaseous medium :	Air or helium
Total pressure:	0.05 to 0.6 Torr
Electron gun voltage:	0.6 to 5 kV
Electron gun current:	5 to 25 mA
Cathode to substrate spacing:	3 to 20 cm.
Transmission mask-to-substrate spacing:	typically 30 μm.

posure due to the oxidation of the carbon-based polymer by oxygen neutrals and ions from the beam-created plasma.

In patterning experiments the polymer films were differentially exposed by placing a shadow or stencil mask in the path of the soft-vacuum electron beam. Fig. 9(a) shows the plane view of the hexagonal-shaped transmission mask and Fig. 9(b) shows the plane view of the relief pattern replicated on PMMA in the self-development mode. Feature sizes of 7 μm are easily duplicated in the presence of 100 mtorr of ambient gas. However, the relief image in the polymer film never showed complete development regardless of the increases in the electron dose (higher discharge current, longer exposure time, lower ambient pressure, and smaller sample-to-cathode distance). A dark layer on top of the polymer is observed to form, which prevents further etching, and is most likely a surface layer which has undergone chemical changes that render it much more oxidation-resistant.

In order to achieve a full relief pattern definition, a two-step dry processing sequence was carried out. After the polymer film layer is exposed to the soft-vacuum electron beam through a stencil mask, the stencil mask was removed and the previously exposed polymer layer was flood-irradiated by low-voltage electrons. It should be noted, however, that when high pressures (>1 torr) and low gun voltages (<1 kV) are used to perform the dry development step in the lithographic process, the discharge characteristics are similar to those of normal glow discharge. A negative pattern is formed due to the differential etch rate between the exposed region and the unexposed region. To obtain the largest differential etch rate, low pressure (<0.2 torr) and high gun voltage (>3 kV) are preferred for exposure, while high pressure (>1 torr) and low gun voltage (<1 kV) are preferred for development. This two-step patterned exposure and dry development results in the replication of mask features such as those shown in Fig. 10. The plan view of the relief pattern (Fig. 10(b)) can be compared to the original mask pattern (Fig. 10(a)).

B. Resist Patterning By Pulsed Electron-Beam Exposure

Due to the intense peak powers, simultaneous exposure and self-development were achieved. Typical pulsed plasma-beam operating conditions for the lithographic experiments carried out in the apparatus of Fig. 2 are listed in Table II. Fig. 11 summarizes the polymer self-development characteristics obtained via pulsed exposure for four common microelectronic polymers.

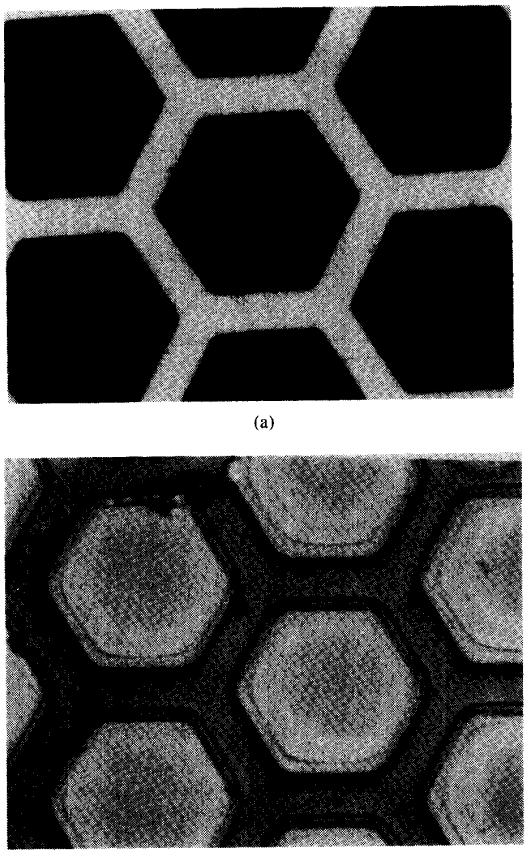

(a)

(b)

Fig. 9. PMMA pattern replication by self-development process. (a) Plane view of characteristic mask features. (b) Plane view of relief pattern.

A thin metal foil with a 2-mm-diam hole was used as the transmitting element to determine the material removed from the exposed area, as compared to the unexposed area. Polymer thickness was measured before and after electron exposure on a stylus displacement instrument. Note that (i) areas of the polymer films are not completely etched, and (ii) the material removal rate increases with the number of pulses used until saturation occurs.

Plane-view microphotographs of polymer films patterned directly by the pulsed electron beam without the development step are shown in Fig. 12. In Fig. 12(a), patterning of Poly (1-hexene-sulfone) was achieved using a 0.38-mm-thick silicon membrane with submicron size (0.5 μm) features as an electron transmitting mask and exposed to a 10 pulse, 25-keV electron beam in helium at 70 mtorr. These small feature sizes were replicated in the polymer relief image. Fig. 12(b) shows the erosion of Poly (N-vinyl carbazole) with a single pulse at 40-mtorr air using a scanning electron microscope grid as a transmission mask with 5-μm features. Fig. 12(c) shows the self-development pattern on PMMA using the same mask, fol-

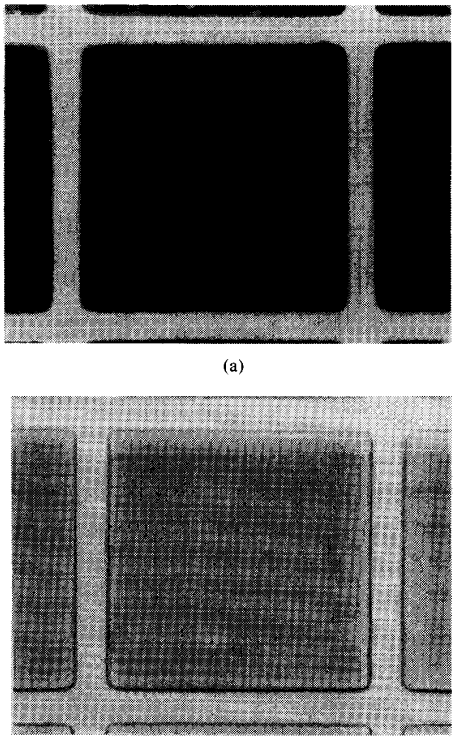

Fig. 10. Polyamic acid is exposed and developed via a two-step process to replicate negative tone patterns. (a) Shadow mask. (b) Negative pattern.

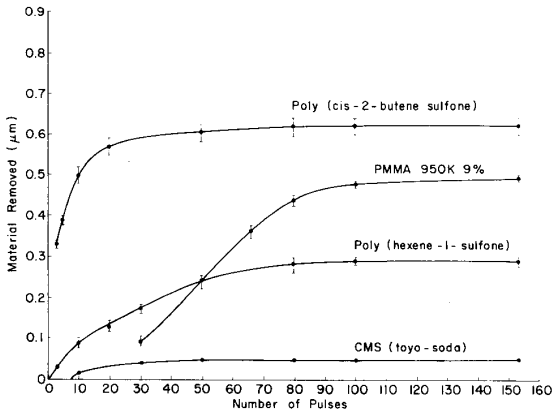

Fig. 11. Partial self-development of four selected polymers versus the number of soft-vacuum electron-beam pulses employed.

TABLE II
EXPERIMENTAL CONDITIONS FOR ESTABLISHING THE PULSED ELECTRON BEAM

Gaseous medium:	Air or helium
Pressure:	0.05 to 0.08 Torr
Electron gun voltage:	25 to 28 kV
Cathode to substrate spacing:	8 cm
Transmission mask-to substrate spacing:	typical 30 μm

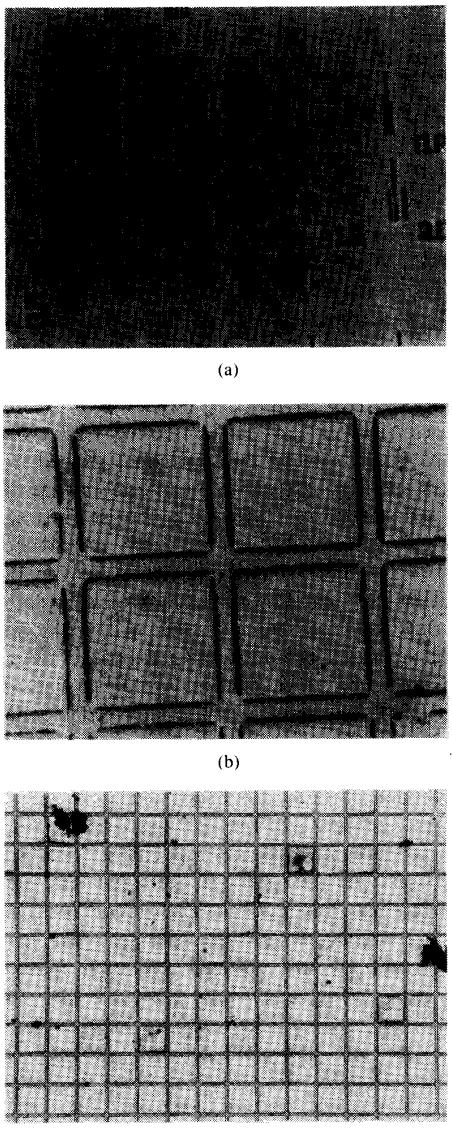

Fig. 12. Plane view microphotographs of self-developed patterns on polymers following exposure to pulsed electron beams. (a) Poly (hexene-1-sulfone) resist on silicon substrate. (b) Aromatic resist, poly (N-vinyl carbazole) on the glass. (c) Self-developed pattern in a 1.8-μm thick PMMA.

lowing proximity exposure to 100 pulses at a 25-keV electron beam produced in air at 30 mtorr. The feature sizes shown in both Fig. 12(b) and (c) are ~5 μm, but Fig. 12(b) is at a higher magnification. In the case of PMMA for which cross-sectional SEM micrographs could also be obtained, the wall profiles were sloped at ~45°.

Wet development experiments were carried out primarily with PMMA, using a standard developer of 1:1 Methyl Isobutyl Ketone to Isopropyl Alcohol. PMMA films were spin coated on silicon wafers from PMMA (molecular weight = 950 000) dissolved in chloroben-

zene. The time required to perform wet development was strongly affected by the electron-beam treatment. A single pulse (<1 μs) was sufficient to expose the PMMA film for long development times, and 3 to 5 pulses were required for shorter wet development durations. When the number of pulses exceeded 20, partial self-development took place. Fig. 13(a) shows the replication of relief image features onto PMMA (~ 1.5 μm in thickness) when using the SEM transmission mask (width of the lines is 7 μm) as a stencil mask. The corrugations on the sidewalls of the resist correspond to the jagged edge of the source mask. Fig. 13(b) provides a higher magnification of the sidewall. Notice the vertical sidewalls and high contrast in the relief image. Films were exposed in the proximity mode using a ~ 25-μm spacer between the mask and polymer surface. Fig. 14 shows a plane view of the fine-line relief image replication (~ 0.5 μm) in a ~ 3-μm-thick PMMA film.

Self-development was observed in both continuous and pulsed beam exposure. In the wet development following the beam exposure experiments, one can see that a much better result is achieved in the pulsed beam exposure, due mainly to deeper penetration into the resist by electrons with much higher energy.

C. Resist Hardening by Pulsed Electron Beam

Soft-vacuum electron-beam hardening experiments were carried out on films of AZ-type photoresist and MacDermid deep UV resist using the apparatus of Fig. 2. The experiments consisted of three steps: Conventional film preparation and pattern definition, soft-vacuum pulsed electron-beam hardening, and high-temperature cycling. It is during this latter step that unhardened resist will distort. We quantitatively evaluated the success or failure of the hardening process by heating the hardened resist at a predetermined high temperature (200° to 350° depending on the resist) for various times (10 to 30 min). As a baseline comparison we also used relief images hardened by UV exposure.

AZ-type resist patterns, 3.5 μm in thickness, on silicon wafers were exposed to 30, 50, 100, 150, and 200 pulses of 25-kV electrons produced in 50 mtorr of dry air. The resist-coated silicon wafers were placed 8 cm from the cold cathode face during irradiation. For comparison purposes, a separate group of resist patterns was exposed to a deep UV photostabilization source for 7.5 min, with an estimated UV dose of 6 J/cm^2. The unexposed resist patterns, the deep UV exposed resist patterns, and the electron-irradiated resist patterns were all temperature-cycled at 250°C for 10 min, and these results are shown in Fig. 15. Fig. 15(a) shows the distortion of the unhardened resist patterns expected after exceeding the resist reflow temperature. Fig. 15(b) shows the excellent stability of the pulsed electron-beam (25 keV, 200 pulses)-hardened resist patterns, and Fig. 15(c) shows the partial thermal flow of the resist features of deep UV hardened resist. In the deep UV hardening process of this experiment, even greater distortion of large-size (more than 10 μm) patterns

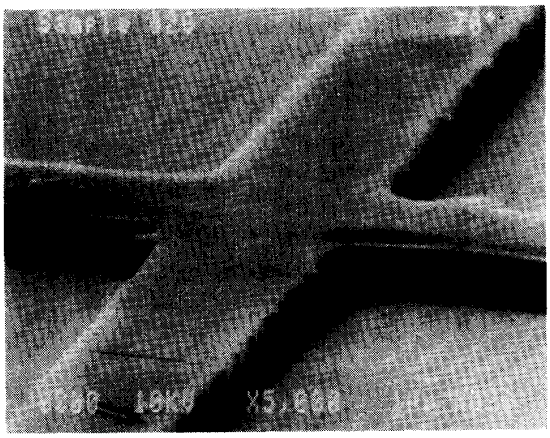

(a)

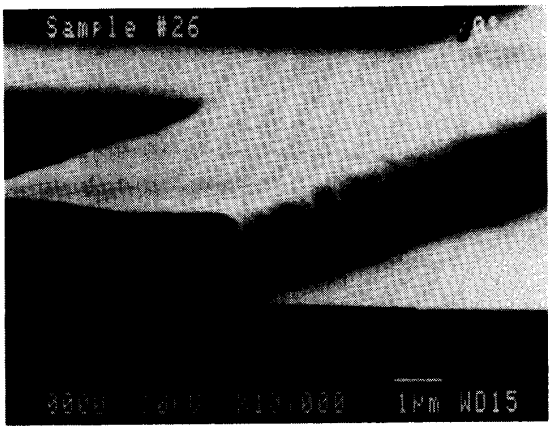

(b)

Fig. 13. SEM micrography of wet-developed pattern in PMMA. (a) Plane view at 70°. (b) Cleaved section at 80°.

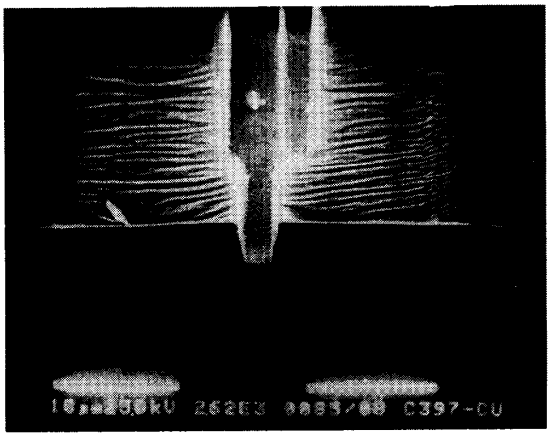

Fig. 14. Plane-view SEM of fine relief image line through a submicron stencil mask placed in proximity (25 μm) to the substrate.

was observed under 250°C treatment for 10 min, but micrometer-features on the same samples did not flow or distort. Additionally, extensive reticulation was observed on

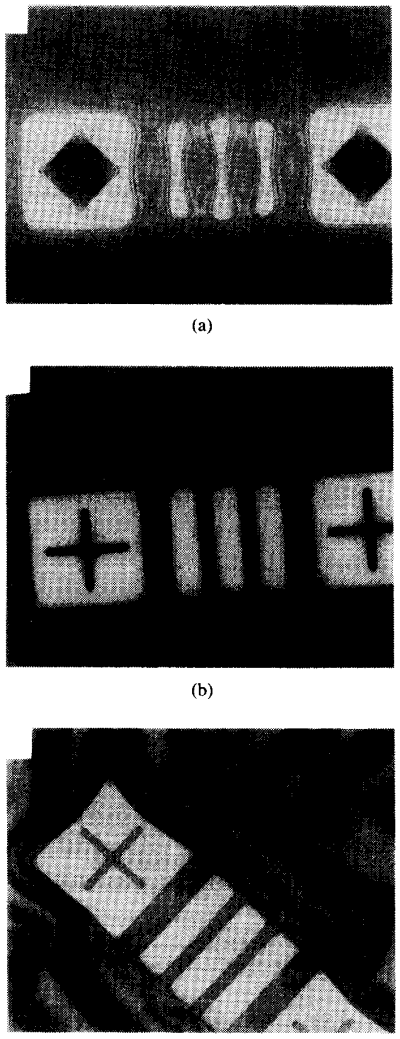

(a) (b) (c)

Fig. 15. Temperature-time-induced pattern distortion following hardening of AZ-type photoresist. (a) Gross distortion of unhardened resist after *T-t* heat treatment. (b) Stable resist profiles of pulsed, soft-vacuum, electron-beam hardened resist profiles after *T-t* heat treatment. (c) Deep UV hardened resist profiles after *T-t* heat treatment.

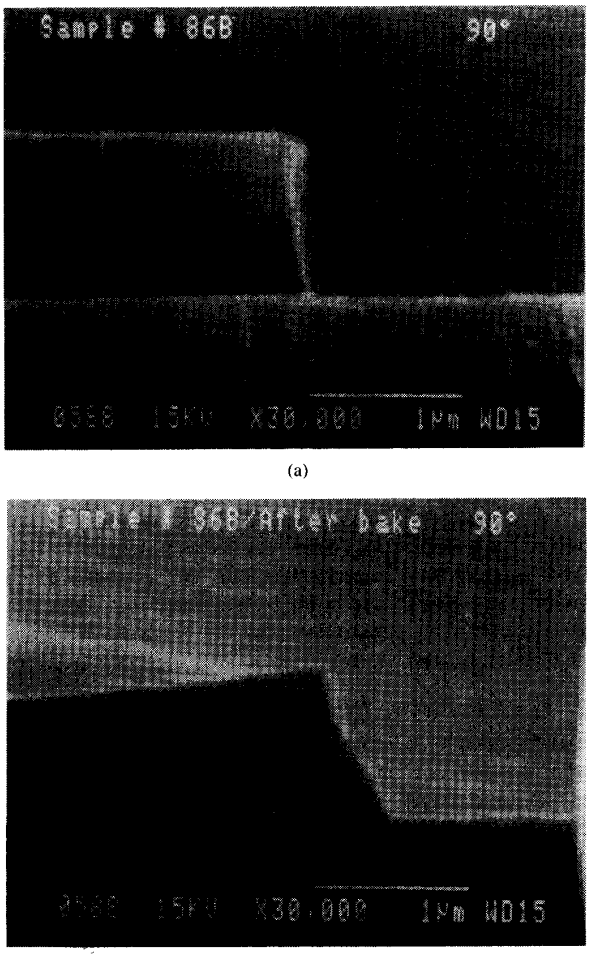

(a) (b)

Fig. 16. Temperature-time-induced pattern distortion following the hardening of the MacDermid resist by UV emission from a high-pressure mercury lamp. (a) SEM micrography of the resist profile before *T-t* heat treatment. (b) SEM micrograph of the resist after heat treatment.

large-area resist images. These comparative experiments clearly demonstrate the advantages of the electron-beam hardening process.

Photolithographic relief patterns were next obtained by using MacDermid (MACD-914) resist coated on silicon wafers. One-half of the resist pattern was shadowed with an electron blocking mask, and the other half of the resist patterns was exposed to the hardening effect of the soft-vacuum pulsed electron beam. Unexposed and exposed (hardened) resist regions were chosen from two neighboring points in order to achieve a comparison which was independent of the local variations of the polymer film that are known to occur. The improved preservation of relief images of developed resist by the pulsed electron-beam hardening was demonstrated. A comparison was also made between deep UV hardening and pulsed electron-beam hardening. Fig. 16(a) and (b) shows micrographs of UV-hardened MacDermid resist profiles using a 900-W Hg lamp for 1 h, before (Fig. 16(a)) and after (Fig. 16(b)) a 200°C bake for 10 min. There is evidence of top surface hardening in the form of a hardened crust.

A comparison between low-energy cw electron-beam exposure for hardening and pulsed higher energy electron-beam exposure for hardening was made in Fig. 17. The total doses are nearly the same in the pulsed and continuous electron-beam hardening, but the electron energies are quite different. Fig. 17(a) shows the scanning electron micrograph of a cleaved section of an unhardened resist layer. Fig. 17(b) shows a micrograph of the same layer when heated at 200°C for a half hour. Extensive

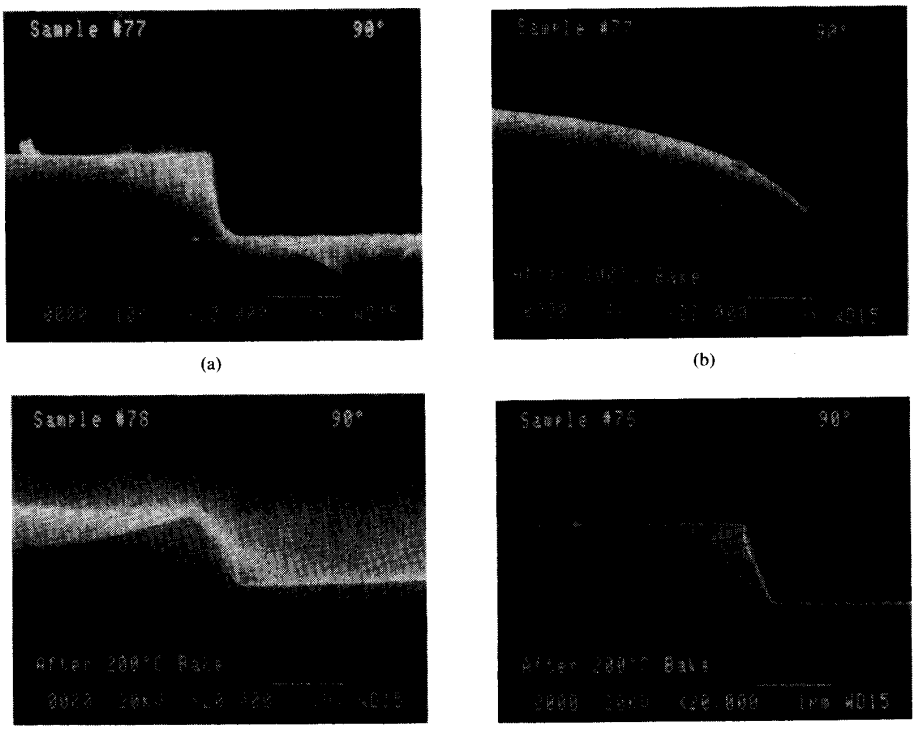

Fig. 17. Temperature-time-induced pattern distortion following the hardening of the MacDermid resist with a low-voltage cw electron beam and a higher voltage pulsed electron beam. (a) Cleaved resist profile of unhardened resist. (b) Effect of *T-t* heat treatment on the unhardened resist profile. (c) Resist profile of cw low-voltage electron-beam hardened resist after heat treatment. (d) Resist profile of higher voltage, pulsed electron-beam hardened resist after *T-t* heat treatment.

flow resulting in the gross rounding of the edge can be clearly seen. 28-kV electrons produced in the apparatus shown in Fig. 2 irradiated the sample of Fig. 17(d) with 70 pulses, while the sample of Fig. 17(c) was then exposed to ~4.5-kV electrons produced in 75-mtorr air for 1 s with an effective electron current of 7.5 mA. Fig. 17(c) shows the SE micrograph of a continuous low-voltage electron-beam-hardened layer after the same heat treatment. There appears to be some superficial hardening, but the pattern is still distorted. Fig. 17(d) shows the SE micrographs of the pulsed electron-beam-hardened resist patterns that indicate excellent pattern stability under the same thermal cycle. The better hardening result by the pulsed electron beam than that by the continuous electron beam is because of the deeper penetration of high-energy electrons.

IV. Conclusions

Kilovolt electron beams were produced using a continuous and a pulsed gas discharge in soft vacuum (0.05 torr $< p <$ 0.5 torr), passed through proximity transmission masks to impinge on selected polymer films. Electron irradiation of polymer films results in partial gasification and associated film removal. The single-step soft-vacuum electron-beam exposure and partial etching process (i.e., self-development) is limited by a saturation phenomena that necessitates an additional development process to achieve a complete image definition in the polymer film. A pulsed electron beam at 25 keV, 2.5-cm diam in 30-mtorr dry air was used as an exposure tool. The spontaneous removal rates of several self-developing polymers have been measured. A replication capability of ~0.5-μm feature size with an aspect ratio of 1 : 6 in the resist has been demonstrated using sequential exposure through soft contact (mask-to-polymer surface spacing = 25 μm), followed by wet development. The 25-keV pulsed electron beam is also effective in hardening resist relief patterns in resist/polymer materials. Resist thickness ranging from 0.5 to 3.5 μm has been shown to uniformly harden under the pulsed electron-beam irradiation conditions.

The soft-vacuum approach suffers less from undesired mask heating and mask charging problems as compared to the transmission masks used in hard vacuum with either thermonic electron or ion beams. The use of a cold cathode and large pumping speed greatly reduce the cathode contamination problem. Although the soft-vacuum method may not be suitable for submicron pattern delineation due mainly to the unavailability of submicron stencil masks, it may provide a low-cost alternative for pack-

aging lithography in which the resist thickness is substantial, line widths are larger, and registration requirements are not so critical. The 25-kV electrons can harden effectively at ~10-μm-thick polymers and may be especially well-suited for packaging lithography.

Acknowledgment

The authors thank C. Messer, M. Henderson, and T. Potts of the Hewlett Packard Corporation, Fort Collins, CO, for the excellent SEM micrographs. They also thank Dr. Moir of the Los Alamos National Laboratory for electron dose measurements and Dr. Rocca for lending a Tektronix 7104 oscilloscope.

References

[1] D. R. Herriott, R. J. Collier, D. S. Alles, and J. W. Stafford, *IEEE Trans. Electron Devices*, vol. ED-22, no. 7, p. 385, 1975.
[2] R. Ward, A. R. Franklin, P. Gould, and M. J. Plummer, *J. Vac. Sci. Technol.*, vol. 19, no. 4, p. 966, Nov.-Dec. 1982.
[3] M. J. Bowden and L. F. Thompson, "Vapor development of poly (Olefin sulfone) resists," *Polymer Eng. Sci.*, vol. 14, p. 525, 1974.
[4] H. Ito and C. G. Wilson, "Applications of photoinitiators to the design of resists for semiconductor manufacturing," in *Polymers in Electronics* (Amer. Chem. Soc. Symp., Ser. 242), T. Davidson, Ed. New York: Amer. Chem. Soc. Symp., 1984, pp. 11-24.
[5] H. Hiraoka, "All dry lithographic processes and mechanistic studies with poly (methacrylonitrile) and related polymer," *J. Electrochem. Soc.*, vol. 128, p. 1065, 1981.
[6] M. Yamada, J. Tamano, K. Yoneda, S. Morita, and S. Hattori, "Electron beam vacuum lithography using plasma co-polymerized MMA-TMT resist," *Japan J. Appl. Phys.*, vol. 21, no. 5, p. 768, 1982.
[7] G. N. Taylor, "X-ray resist materials," *Solid State Technol.*, vol. 23, no. 5, p. 73, 1980.
[8] J. N. Smith, H. G. Hughes, J. V. Keller, W. R. Goodner, and T. E. Wood, "A production viable plasma developable photoresist," *Semicond. Int.*, vol. 2, no. 12, p. 41, 1979.
[9] J. Krishnaswamy, L. Li, and G. J. Collings, in *Proc. Colorado Microelectron. Conf. (CMC-86)* (Colorado Springs), 1986, p. 58.
[10] R. Srinivasan *et al.*, presented at the Conf. on Lasers and Electrooptics, Baltimore, May 17-20, 1983.
R. Srinivasan and V. Mayne Banton, *Appl. Phys. Lett.*, vol. 41, p. 576, 1982.
[11] P. Burggraaf, *Semicond. Int.*, vol. P84, Apr. 1987.
[12] J. J. Grunwald, Advances in resist technology and processing III, *SPIE*, vol. 631, 1986.
Semicond. Int., vol. P4, Apr. 1988.
[13] H. Hiraoka and J. Pacansky, *J. Electrochem. Soc.*, vol. 128, p. 2645, 1981.
[14] W. H. L. Ma, U.S. Patent 4 187 331.
[15] K. Hashimoto, K. Yamashita, K. Kawakita, and N. Nomura, presented at the Electrochem. Soc. Meet., Honolulu, HI, Oct. 1987, Paper 734.
[16] W. Moreau, *Microcircuit Eng.*, vol. 83, p. 320, 1983.
[17] H. Hiraoka and J. Pacansky, *J. Vac. Sci. Technol.*, vol. 19, no. 4, p. 1132, 1981.
[18] K. J. Orvek and M. L. Dennis, presented at the SPIE Conf. on Microlithography, Santa Clara, CA, 1987, Paper 771 47.
[19] H. Hiraoka et *al.*, presented at the Electrochem. Soc. Meet., Symp. on Patterning Sci. Technol., Honolulu, HI, Oct. 18-23, 1987.
J. Krishnaswamy, L. Li, G. J. Collins, H. Hiraoka, and M. A. Caolo, presented at the Fall Meet. Materials Res. Soc., Symp. B., Boston, Dec. 1-6, 1987, paper B7.9.
[20] W. H.-L. Ma, *SPIE Submicron Lithogr.*, vol. 333, p. 19, 1982.
[21] C. Johnson, Jr., S. M. Ku, H. V. Lillja, and E. J. Pan, U.S. Patent 3 920 483.
[22] J. M. Moran and G. N. Taylor, *J. Vac. Sci. Technol.*, vol 19, no. 4, p. 1127, 1981.
[23] R. Srinivasan, *IBM J. Res. Develop.*, RC 9177, 1981.
R. Srinivasan and B. Braren, *J. Polymer Sci.*, vol. 22, p. 2601, 1984.
[24] J. Krishnaswamy, L. Li, G. J. Collins, H. Hiraoka, and M. A. Caolo, "Science and Technology of Microfabrication," in *Proc. Materials Res. Soc.*, 1987, p. 91.
IBM Int. Rep., RJ 5441, 55690, 1986.
[25] A. Novembre and T. N. Bowmer, in *Materials for Microlithography* (ACS Symp. Ser. 266), C. G. Wilson, L. F. Thomson, and J. M. J. Frechet, Eds. Washington, DC: ACS, 1984, ch. 11, p. 241.
[26] H. Dreicer, *Phys. Rev.*, vol. 117, no. 2, p. 329, 1960.
[27] J. Geiger, *Z. Phys.*, vol. 175, p. 530, 1963.
J. Geiger, *Z. Phys.*, vol. 177, p. 138, 1964.
[28] B. Shi, J. Meyer, Z. Yu, and G. J. Collins, *IEEE Trans. Plasma Sci.*, vol. PS-14, p. 523, 1986.
R. J. Carman and A. Maitland, *J. Phys.*, vol. D20, p. 1021, 1987.
[29] H. F. Ranea-Sandoval, N. Reesor, B. T. Szapiro, C. Murray, and J. J. Rocca, *IEEE Trans. Plasma Sci.*, vol. PS-15, no. 4, p. 361, 1987.
[30] B. B. O'Brien, Jr., *Appl. Phys. Lett.*, vol. 22, p. 503, 1973.
[31] G. G. Isaacs, D. L. Jordon, and P. J. Dooley, *J. Phys. E. Sci. Instrum.*, vol. 12, p. 115, 1979.
[32] P. Gill and C. E. Webb, *J. Phys.*, vol. D-10, p. 299, 1977.
[33] Z. Yang *et al.*, to be published.
[34] S. W. Downey, L. A. Builta, R. L. Carlson, S. J. Chuchlewski, and D. C. Moir, *J. Appl. Phys.*, vol. 60, no. 10, p. 3460, 1986.

*

Lumin Li was born in China on July 3, 1952. He graduated from the Electronics Department in 1978, and received the Master's Degree of Technology in 1982 from the Nanjing Insitute of Technology. He is currently a Ph.D. degree candidate at Colorado State University, Fort Collins. His thesis work has involved the soft lithographic processes. His research interests are in plasma physics, gas lasers, metal vapor ion lasers, spectroscopy, and vacuum technology.

*

Jayaram Krishnaswamy is a Researcher Assistant Professor in the Department of Materials Science and Engineering at North Carolina State University, Raleigh. He enjoys working in the area of gas discharges and their applications. He holds several patents and has written in the areas of high current discharge, laser discharge, laser initiated plasma, sustained discharge, pulsed electron beams, X ray, etc. Presently he is working on laser CVD and laser CVD for superconducting and super-hard thin-film applications.

Professor Krishnaswamy is a member of the MPS, SPIE, PE, and Electrochemical Society.

*

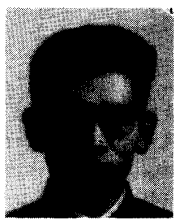

Zengqi Yu (SM'89) was born in China on November 26, 1941. He graduated in physics from Fudan University, Shanghai, and received the M.S. and Ph.D. degrees in electrical engineering from Colorado State University, Fort Collins.

He was teaching and performing experimental research at Fudan University during 1965-1984, and has been doing research at Colorado State University since 1980. His research interests are in soft-vacuum electron-beam sources and their applications to microelectronic film processes, gas lasers, metal vapor ion lasers, laser ablation for film coating, magnetron sputtering for fiber coating, plasma physics, spectroscopy, and vacuum physics.

Dr. Yu is a member of several academic societies.

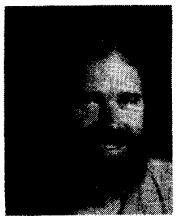

George J. Collins (S'62–M'72–SM'75–F'87) graduated from Yale University, New Haven, CT.

He is a Professor of Electrical Engineering at Colorado State University, Fort Collins. He has served as a Consultant to both industry and government, including Bell Laboratories, NCR, Lawrence Livermore National Laboratory, the National Bureau of Standards, Lasertechnics (Albuquerque NM), and the Applied Electron Corporation (Santa Clara, CA). Prior to joining Colorado State University, he was a Research Associate at the Dunham Laboratory, Oxford University, and a Visiting Scientist under the U.S.–Japan Cooperative Science Program at Nagoya University. He is the author of more than 100 technical papers.

Dr. Collins is a member of the American Physical Society, Eta Kappa Nu, Sigma Xi, Sloan Foundation Fellow (Physics), and is a recipient of the Halliburton Award.

*

Hiroyuki Hiraoka was born and educated in Kyoto, Japan. He obtained the Ph.D. degree from Kyoto University in 1959, and did postdoctoral work at the University of California, Los Angeles, and the University of California, Berkeley, in 1960 to 1964.

He did research work at the Central Laboratory of Teijin Limited, Tokyo, Japan. He joined the IBM T.J. Watson Research Laboratory in 1966 as a Research Staff Member, and moved to the IBM San Jose Research Laboratory in 1971 and presently to the IBM Almaden Research Center. He has studied in various fields of chemistry, including photochemistry; since 1971 he has been involved in radiation and photochemical studies related to electron-, ion-, X ray, and photolithographies.

*

Mary Ann Caolo was born in New York. She received the B.S. (chemistry, 1973) degree from Fordham University, Bronx, NY, and the Ph.D. (chemistry, 1980) degree from Colorado State University, Ft. Collins.

In 1981 she joined the Hewlett Packard Corporation, Ft. Collins, as a member of the technical staff of the Colorado Integrated Circuits Division. She has worked in several areas, including material analysis, and etch and photolithography groups in the manufacture of IC's for the Hewlett Packard work stations. Since 1986 she has been a Faculty Affiliate in the Department of Electrical Engineering at Colorado State University. She has collaborated on soft *e*-beam patterning and teaches an introductory class in microlithography.

Dr. Caolo is a member of the American Chemical Society, the American Vacuum Society, and the Electrochemical Society.